Spin injection and detection in magnetic nanostructures

S. Takahashi and S. Maekawa
Institute for Materials Research, Tohoku University, Sendai 980-8577, Japan
(Received 5 November 2002; published 28 February 2003)

We study theoretically the spin transport in a nonmagnetic metal connected to ferromagnetic injector and detector electrodes. We derive a general expression for the spin accumulation signal which covers from the metallic to the tunneling regime. This enables us to discuss recent controversy on spin injection and detection experiments. Extending the result to a superconducting device, we find that the spin accumulation signal is strongly enhanced by opening of the superconducting gap since a gapped superconductor is a low carrier system for spin transport but not for charge. The enhancement is also expected in semiconductor devices.

DOI: 10.1103/PhysRevB.67.052409 PACS number(s): 72.25.Ba, 72.25.Hg, 72.25.Mk, 73.40.Gk

There has been considerable interest recently in spin transport in magnetic nanostructures.[1] The spin polarized electrons injected from ferromagnets (F) into nonmagnetic materials (N) such as a normal metal, semiconductor, and superconductor create nonequilibrium spin accumulation in N.[2–12] The efficient spin injection, accumulation, and transport are central issues to be explored in manipulating the spin degree of freedom of the electron. Johnson and Silsbee[3] have demonstrated that the injected spins penetrate into N over the spin-diffusion length of μm scale using the spin injection and detection techniques in $F1/N/F2$ trilayer structures. Very recently, Jedema *et al.* have made a permalloy/copper/permalloy (Py/Cu/Py) structure[4] and observed spin accumulation at room temperature. Subsequently, they have shown that the efficiency of spin injection and accumulation is greatly improved in a cobalt/aluminum/cobalt (Co/I/Al/I/Co) structure with tunnel barriers (I).[5]

In this paper, we study the spin injection and detection in a device of $F1/N/F2$ structure by taking into account the geometry of nonlocal measurement.[4,5] By proper modeling of the system in the diffusive transport regime, we derive an analytical expression for the spin accumulation signal which covers from the metallic to the tunnel regime. A controversial issue on the analysis of spin accumulation has been raised in the structures of metallic contacts.[13] We discuss the issue based on the present analytical expression. Extending the result to the device containing a superconductor, we find that the spin signal is greatly enhanced by opening of superconducting gap. Large spin signals are also expected in semiconductor devices.

We consider a spin injection and detection device consisting of a nonmagnetic metal N connected to ferromagnets of injector $F1$ and detector $F2$ as shown in Fig. 1. $F1$ and $F2$ are the same ferromagnetic films of width w_F and thickness d_F, and are separated by distance L. N is a normal-metal film of width w_N and thickness d_N. The magnetizations of $F1$ and $F2$ are aligned either parallel or antiparallel. Since the spin-diffusion length λ_N of N [$\lambda_{Cu}\sim 1$ μm,[4] $\lambda_{Al}\gtrsim 1$ μm (Refs. 3, 5, and 6)] is much larger than the length λ_F of F [$\lambda_{Py}\sim 5$ nm (Ref. 14)], we consider the device having dimensions of $\lambda_F \ll (d_N, d_F) \ll (w_N, w_F) \ll \lambda_N$. This situation, which corresponds to the experimental geometry,[4,5] facilitates a description for the spin and charge transport in the device.

The electrical current $\mathbf{j}_\sigma$ for spin channel σ is driven by the electric field $\mathbf{E}$ and the gradient of the carrier density deviation δn_σ from equilibrium: $\mathbf{j}_\sigma = \sigma_\sigma \mathbf{E} - eD_\sigma \nabla \delta n_\sigma$, where σ_σ and D_σ are the electrical conductivity and the diffusion constant. Making use of $\delta n_\sigma = N_\sigma \delta \epsilon_\sigma$ and $\sigma_\sigma = e^2 N_\sigma D_\sigma$ (N_σ is the density of states in the spin subband and $\delta\epsilon_\sigma$ is the shift in the chemical potential of carriers from its equilibrium value) gives $\mathbf{j}_\sigma = -(\sigma_\sigma/e)\nabla \mu_\sigma$, where $\mu_\sigma = \epsilon_\sigma + e\phi$ is the electrochemical potential (ECP) and ϕ the electric potential. The continuity equations for charge and spin in the steady state are $\nabla \cdot (\mathbf{j}_\uparrow + \mathbf{j}_\downarrow) = 0$ and $\nabla \cdot (\mathbf{j}_\uparrow - \mathbf{j}_\downarrow) = -e\,\delta n_\uparrow/\tau_{\uparrow\downarrow} + e\,\delta n_\downarrow/\tau_{\downarrow\uparrow}$, where $\tau_{\sigma\sigma'}$ is the scattering time of an electron from spin state σ to σ'. Using these equations and detailed balancing $N_\uparrow/\tau_{\uparrow\downarrow} = N_\downarrow/\tau_{\downarrow\uparrow}$, one obtains[3,15–19]

$$\nabla^2(\sigma_\uparrow \mu_\uparrow + \sigma_\downarrow \mu_\downarrow) = 0, \tag{1}$$

$$\nabla^2(\mu_\uparrow - \mu_\downarrow) = \lambda^{-2}(\mu_\uparrow - \mu_\downarrow), \tag{2}$$

with the spin-diffusion length $\lambda = \sqrt{D\tau_{sf}}$, where $\tau_{sf}^{-1} = \frac{1}{2}(\tau_{\uparrow\downarrow}^{-1} + \tau_{\downarrow\uparrow}^{-1})$ and $D^{-1} = (N_\uparrow D_\downarrow^{-1} + N_\downarrow D_\uparrow^{-1})/(N_\uparrow + N_\downarrow)$. The material parameters in N are spin *independent*: $\sigma_N^\uparrow = \sigma_N^\downarrow = \frac{1}{2}\sigma_N$, $D_\uparrow = D_\downarrow$, etc., and those in F spin *dependent*: $\sigma_F^\uparrow \neq \sigma_F^\downarrow$ ($\sigma_F = \sigma_F^\uparrow + \sigma_F^\downarrow$), $D_\uparrow \neq D_\downarrow$, etc.

We employ a simple model for the interfacial currents of the junctions. The distribution of the interfacial spin currents is uniform over the contact area $A_J = w_F w_N$ since the λ_N is much longer than w_F and w_N, and ECP has a discontinuous drop at the interface of junction i ($i = 1,2$) asso-

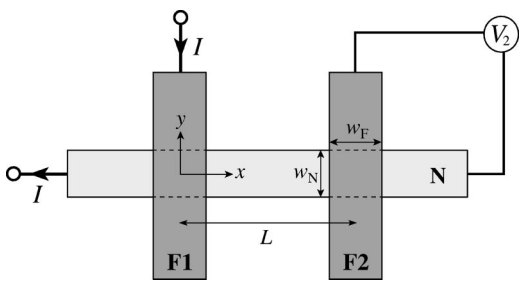

FIG. 1. Basic structure of a spin injection and detection device. The bias current I flows from $F1$ to the left side of N. The spin accumulation at distance L is detected by measuring the spin-dependent voltage V_2 between $F2$ and N.

ciated with the interface resistance R_i.[3,16–19] We neglect the interfacial spin-flip scattering[17,19] for simplicity. The interfacial current I_i^σ across the interface ($z=0$) is given by $I_i^\sigma = (G_i^\sigma/e)(\mu_F^\sigma|_{z=0^+} - \mu_N^\sigma|_{z=0^-})$, where G_i^σ is the interface conductance ($G_i = G_i^\uparrow + G_i^\downarrow = R_i^{-1}$). In the transparent contact ($G_i \to \infty$) the ECPs are continuous at the interfaces, while in the tunneling junction the discontinuity in ECP is much larger than the spin splitting in ECP. The interfacial charge and spin currents are $I_i = I_i^\uparrow + I_i^\downarrow$ and $I_i^s = I_i^\uparrow - I_i^\downarrow$.

When the bias current I flows from $F1$ to the left side of N ($I_1 = I$) and no charge current through the $F2/N$ junction ($I_2 = 0$), the solutions for ECP's that satisfy Eqs. (1) and (2) are constructed as follows. In the N electrode whose thickness and contact dimensions are much smaller than λ_N, μ_N^σ varies only in the x direction: $\mu_N^\sigma(x) = \overline{\mu}_N + \sigma\delta\mu_N$, where $\overline{\mu}_N = (eI/\sigma_N)x$ for $x<0$, $\overline{\mu}_N = 0$ for $x>0$, and $\delta\mu_N = a_1 e^{-|x|/\lambda_N} + a_2 e^{-|x-L|/\lambda_N}$ with the a_1 term being the ECP shift due to spin injection from $F1$ at $x=0$, and the a_2 term being the feedback shift due to the presence of $F2$ at $x=L$. The spin current $j_s = j_\uparrow - j_\downarrow$ flows in the x direction according to $j_s = -(\sigma_N/e)\nabla\delta\mu_N$. The continuity of the spin current at junction i yields $I_i^s = 2(\sigma_N A_N/e\lambda_N)a_i$, where $A_N = w_N d_N$ is the cross-sectional area of N. Note that only the spin current flows in the region of $x>0$ and no charge current there.

In the $F1$ and $F2$ electrodes whose thickness and contact dimensions are much larger than λ_F, the spin splitting of μ_F^σ decays quickly along the z direction, so the solution has the form near the interface ($0<z\lesssim\lambda_F$): $\mu_F^\sigma(z) = \overline{\mu}_F + \sigma b_i(\sigma_F/\sigma_F^\sigma)e^{-z/\lambda_F}$, where $\overline{\mu}_F = (eI/\sigma_F A_J)z + eV_1$ in $F1$ and $\overline{\mu}_F = eV_2$ in $F2$, V_1 and V_2 being the voltage drops $(\overline{\mu}_F - \overline{\mu}_N)/e$ at the interfaces of junctions 1 and 2, respectively. The continuity of the spin currents at the junctions leads to $I_1^s = p_F I - 2(\sigma_F A_J/e\lambda_F)b_1$ and $I_2^s = -2(\sigma_F A_J/e\lambda_F)b_2$, where $p_F = (\sigma_F^\uparrow - \sigma_F^\downarrow)/(\sigma_F^\uparrow + \sigma_F^\downarrow)$ is the current polarization of $F1$ and $F2$. The constants a_i, b_i, and V_i are determined by the continuity condition for the spin and charge currents at the interfaces.

The spin-dependent voltage V_2 detected at $F2$, i.e., the potential difference between the right side of N electrode and the $F2$ electrode, is given by

$$V_2/I = \pm 2\mathcal{R}_N e^{-L/\lambda_N} \prod_{i=1}^{2} \left(\frac{P_J \frac{R_i}{\mathcal{R}_N}}{1-P_J^2} + \frac{p_F \frac{\mathcal{R}_F}{\mathcal{R}_N}}{1-p_F^2} \right) \times \left[\prod_{i=1}^{2} \left(1 + \frac{2\frac{R_i}{\mathcal{R}_N}}{1-P_J^2} + \frac{2\frac{\mathcal{R}_F}{\mathcal{R}_N}}{1-p_F^2} \right) - e^{-2L/\lambda_N} \right]^{-1}, \tag{3}$$

where signs "+" and "−" correspond to the parallel (P) and antiparallel (AP) alignments of magnetizations, $\mathcal{R}_N = \rho_N\lambda_N/A_N$ and $\mathcal{R}_F = \rho_F\lambda_F/A_J$ represent the resistances of N and F with cross sections A_N and A_J and lengths λ_N and λ_F, respectively, and $P_J = |G_i^\uparrow - G_i^\downarrow|/G_i$ is the interfacial current polarization, and $\rho_N = \sigma_N^{-1}$ and $\rho_F = \sigma_F^{-1}$ are the resistivities. The spin accumulation signal is detected as the voltage change $V_s = (V_2^P - V_2^{AP}) = 2|V_2|$ or the resistance change $R_s = V_s/I$ when the magnetizations change from the P to AP alignment.

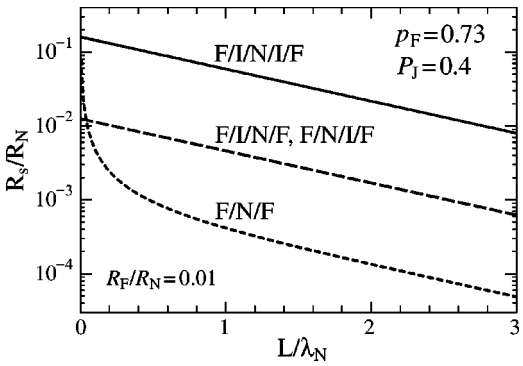

FIG. 2. Spin accumulation signal R_s vs distance L between $F1$ and $F2$. Solid line: $F/I/N/I/F$. Long-dashed line: $F/I/N/F$ and $F/N/I/F$. Short-dashed line: $F/N/F$.

The spin accumulation signal R_s depends on whether each junction is a metallic contact or a tunnel junction. Since $\mathcal{R}_F/\mathcal{R}_N \sim 0.01$ for the typical values ($\rho_F/\rho_N \sim 10$, $\lambda_F/\lambda_N \sim 0.01$, and $A_N/A_J \sim 0.1$),[4] we have the following limiting cases: when both junctions are transparent contact ($R_1, R_2 \ll \mathcal{R}_F$), we have[4,17–19]

$$R_s = \frac{4p_F^2}{(1-p_F^2)^2}\mathcal{R}_N\left(\frac{\mathcal{R}_F}{\mathcal{R}_N}\right)^2 \frac{e^{-L/\lambda_N}}{1-e^{-2L/\lambda_N}}. \tag{4}$$

When one of the junctions is a transparent contact and the other is a tunnel junction, i.e., ($R_1 \ll \mathcal{R}_F \ll \mathcal{R}_N \ll R_2$) or ($R_2 \ll \mathcal{R}_F \ll \mathcal{R}_N \ll R_1$), we have

$$R_s = \frac{2p_F P_J}{(1-p_F^2)}\mathcal{R}_N\left(\frac{\mathcal{R}_F}{\mathcal{R}_N}\right)e^{-L/\lambda_N}. \tag{5}$$

When both junctions are tunneling junctions ($R_1, R_2 \gg \mathcal{R}_N$), we have[3,5]

$$R_s = P_J^2 \mathcal{R}_N e^{-L/\lambda_N}. \tag{6}$$

Note that R_s in the above limiting cases is independent of R_i. Equations (4)–(6) indicate that the resistance mismatch factor ($\mathcal{R}_F/\mathcal{R}_N$) is removed systematically when a transparent contact is replaced with a tunnel junction.[19–22] Thus the maximum spin signal is achieved when all the junctions are tunnel junctions.

Figure 2 show the spin accumulation signal R_s in Eqs. (4)–(6) for $p_F = 0.73$,[14] $P_J = 0.4$,[23] and $\mathcal{R}_F/\mathcal{R}_N = 10^{-2}$.[4] We see that R_s increases by one order of magnitude by replacing a transparent contact with a tunnel barrier. The value $\mathcal{R}_N = 3\ \Omega$,[24] taken from the Py/Cu/Py structure, yields $R_s = 1\ \text{m}\Omega$ at $L = \lambda_N$. If one takes into account the cross-shaped Cu,[4] one expects one-third of the above value, which is in reasonable agreement with the experimental value 0.1 mΩ.[4] In the Co/I/Al/I/Co structure, $\mathcal{R}_N = 3\ \Omega$ is estimated[25] and $R_s = 100\ \text{m}\Omega$ is obtained at $L = \lambda_N$, which is ten times larger than the experimental value 10 mΩ.[5] This

discrepancy may be attributed to the reduction in P_J due to the spin-flip scattering at the barriers.[17,19]

A question arises on whether the contacts of metallic $F1/N/F2$ structures is transparent ($R_i \ll \mathcal{R}_F$)[4] or tunneling-like ($R_i \gg \mathcal{R}_N$).[13,26] The experimental values of Py/Cu [$R_i A_J \sim 5\times10^{-12}$ Ω cm^2,[14] $\rho_F \sim 10^{-5}$ Ω cm,[4] and $\lambda_F \sim 5$ nm (Ref. 14)] yields $R_i \sim \mathcal{R}_F$, which is strictly speaking neither transparent or tunneling-like. However, the values of R_s for $R_i = \mathcal{R}_F$ calculated from Eq. (3) are about two times larger than those for the transparent case in Fig. 2, indicating that the Py/Cu/Py structure lies on the verge of transparent regime. However, depending on sample fabrication processes, there will be cases that belong to the intermediate regime ($\mathcal{R}_F \ll R_i \ll \mathcal{R}_N$), for which one should use

$$R_s = \frac{4P_J^2}{(1-P_J^2)^2}\mathcal{R}_N\left(\frac{R_1R_2}{\mathcal{R}_N^2}\right)\frac{e^{-L/\lambda_N}}{1-e^{-2L/\lambda_N}}. \quad (7)$$

If $R_i \sim \mathcal{R}_N$, then R_s is close to the values of tunneling case, so that the contacts of $R_i \gtrsim \mathcal{R}_N$ belong to the tunneling regime.

The spin injection into a superconductor (S) is of great interest from basic and practical points of views. We show that S becomes a low-carrier system for spin transport by opening of the superconducting gap Δ and the resistivity of the spin current increases below the superconducting critical temperature T_c. In the tunneling device of $F1/I/S/I/F2$, the spin signal would increase due to the increase of $\mathcal{R}_N$ below T_c [see Eq. (6)]. Therefore we investigate in detail how the spin signal is enhanced by opening of Δ. In the following, we consider the situation where the spin splitting of ECP, the maximum of which is $\delta\mu_N(0) \sim \frac{1}{2}eP_J\mathcal{R}_N I$, is smaller than Δ, i.e., $I < 2\Delta/(eP_J\mathcal{R}_N)$, for which the suppression of Δ due to spin accumulation can be neglected.[27] We also neglect charge imbalance created by injection of quasiparticle (QP) charge into S, which originates from the conversion of injected QP's into condensate, and produces the excess voltage due to charge accumulation at $F2$.[28] However, the effect is spin independent and does not contribute to R_s.

In the superconducting state, the equation for the spin splitting ($\mu_\uparrow - \mu_\downarrow$) is the same as Eq. (2) with λ_N in the normal state,[29] which is intuitively understood as follows. Since the dispersion curve of the QP excitation energy is given by $E_k = \sqrt{\epsilon_k^2 + \Delta^2}$ with one-electron energy ϵ_k, the QP's velocity $\tilde{v}_k = (1/\hbar)(\partial E_k/\partial k) = (|\epsilon_k|/E_k)v_k$ is slower by the factor $|\epsilon_k|/E_k$ compared with the normal-state velocity $v_k (\approx v_F)$. By contrast, the impurity scattering time $\tilde{\tau}_{\sigma\sigma'} = (E_k/|\epsilon_k|)\tau_{\sigma\sigma'}$[30] is longer by the inverse of the factor. Then, the spin-diffusion length $\lambda_S = (\tilde{D}\tilde{\tau}_{sf})^{1/2}$ in S with $\tilde{D} = \frac{1}{3}\tilde{v}_k^2\tilde{\tau}_{imp}$ and $\tilde{\tau}_{imp}^{-1} = \Sigma_{\sigma'}\tilde{\tau}_{\sigma\sigma'}^{-1}$ results in $\lambda_S = \sqrt{D\tau_{sf}} = \lambda_N$ owing to the cancellation of the factor $|\epsilon_k|/E_k$. Consequently, the spin splitting in S has the same form of solution as in N.

Utilizing the so-called semiconducting picture for electron tunneling between F and S, the charge and spin currents across junction 1 are calculated as $I = \tilde{G}_T V$ and $I_1^s = P_J\tilde{G}_T V$ at low bias V ($= V_1 < \Delta$),[31] and those across junction 2 are $I_2 = \tilde{G}_T[V_2 - P_2\delta\mu_N(L)/e] = 0$ and $I_2^s = P_2\tilde{G}_T V_2$. Here, P_2 takes P_J ($-P_J$) for the P (AP) alignment, $\tilde{G}_T = \chi_s(T)G_T$ is the tunnel conductance in the superconducting state, and $\chi_s(T)$ is the Yosida function[32] which represents the reduction of the tunnel conductance by opening of Δ below T_c.

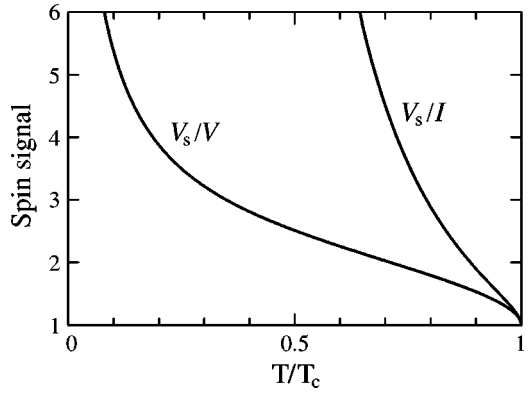

FIG. 3. Temperature dependence of the spin signals $R_s = V_s/I$ and V_s/V in a $F/I/S/I/F$ structure. The values of the spin signal are normalized to those at the superconducting critical temperature T_c.

The spin accumulation in S is determined by balancing the spin injection rate with the spin-relaxation rate: $I_i^s + e(\partial\mathcal{S}_i/\partial t)_{sf} = 0$, where $\mathcal{S}_i$ is the total spins accumulated in S by spin injection through junction i. At low temperatures the spin relaxation is dominated by the spin-flip scattering via the spin-orbit interaction $\mathcal{H}_{so}$ at nonmagnetic impurities or grain boundaries. The scattering matrix elements of $\mathcal{H}_{so}$ over quasiparticle states $|\mathbf{k}\sigma\rangle$ with momentum $\mathbf{k}$ and spin σ has the form: $\langle \mathbf{k}'\sigma'|\mathcal{H}_{so}|\mathbf{k}\sigma\rangle \propto i(u_{k'}u_k - v_{k'}v_k)[\boldsymbol{\sigma}_{\sigma'\sigma}\cdot(\mathbf{k}\times\mathbf{k}')]$, where $\boldsymbol{\sigma}$ is the Pauli spin matrix and $u_k^2 = 1 - v_k^2 = \frac{1}{2}(1 + \epsilon_k/E_k)$. Using the golden rule formula,[31] we can calculate $(\partial\mathcal{S}_i/\partial t)_{sf}$ and obtain $I_i^s = [2f_0(\Delta)/(e\mathcal{R}_N)]a_i$, where $2f_0(\Delta)$ represents the QP populations and $f_0(\Delta) = 1/[\exp(\Delta/k_BT) + 1]$.

From the matching condition of the spin currents across the barriers, we obtain the spin signal R_s in the superconducting state

$$R_s = V_s/I = \frac{1}{2f_0(\Delta)}P_J^2\mathcal{R}_N e^{-L/\lambda_N}. \quad (8)$$

If the $I-V$ characteristics, $I = \chi_s(T)V/R_T$, are used,

$$V_s/V = \frac{\chi_s(T)}{2f_0(\Delta)}P_J^2\frac{\mathcal{R}_N}{R_T}e^{-L/\lambda_N}. \quad (9)$$

The above results are obtained from those of the normal state by the scaling $\rho_N \to \rho_N/[2f_0(\Delta)]$ and $R_T \to R_T/\chi_s(T)$. Equation (8) is interpreted as follows: The spin-current density in S is given by $j_s = -(\sigma_N/e)\ 2f_0(\Delta)\nabla\delta\mu_N$,[33] where the effective conductivity $2f_0(\Delta)\sigma_N$ decreases due to the decrease of QP populations by opening the gap Δ below T_c. The boundary condition that the injected spin current $P_J I$ is equal to $2j_s(0^+)A_N$ yields $\delta\mu_N \approx \{eP_J I\mathcal{R}_N/[2f_0(\Delta)]\}e^{-|x|/\lambda_N}$. The decrease of the effective conductivity is compensated by the increase of $\delta\mu_N$ to maintain the same spin injection in the constant I, and therefore R_s in-

creases as $\frac{1}{2}f_0^{-1}(\Delta)$ below T_c. Note that the T-dependent factor in Eq. (9) is the same as that in the spin-relaxation time $\tau_s=[\chi_s(T)/2f_0(\Delta)]\tau_{sf}$,[34] which is derived from $(\partial\mathcal{S}/\partial t)_{sf}=-\mathcal{S}/\tau_s$.

Figure 3 shows the temperature dependence of $R_s=V_s/I$ and V_s/V. The values are normalized to those at T_c. The strong increase of V_s/I reflects the T dependence of the resistivity of the spin current below T_c. The signal V_s/V increases with the same T dependence as $\tau_s(T)$, indicating that the spin-relaxation time in S is directly obtained by measuring V_s vs T at constant V. To test these predictions, it is highly desirable to measure V_s of Co/I/Al/I/Co structures[5] by lowering T below T_c.

A large enhancement of spin signals is also expected in degenerate semiconductors, because the resistivity is much larger compared with normal metals and the spin-diffusion length is relatively long. In degenerate semiconductors, the spin current is given by $j_s=-\mu_m n_c \nabla_x(\mu_\uparrow-\mu_\downarrow)$, where μ_m is the mobility and n_c the carrier concentration. For Si-doped GaAs with $n_c=10^{18}$ cm^{-3} and $\mu_m=2\times10^3$ cm^2/V s at room temperature,[35] $\rho_N=1/(e\mu_m n_c)=0.1\ \Omega$ cm. For (Mn,Ga)As, $\rho_F=0.01\sim0.1\ \Omega$ cm.[36] It follows from Eq. (5) that $R_s\propto\rho_F$ for a (Ga,Mn)As/I/N/(Ga,Mn)As device, and from Eq. (6) that $R_s\propto\rho_N$ for a $F1$/I/GaAs($n-$type)/I/$F2$ device. Therefore we expect that R_s is larger by several orders of magnitude than that of metal case. This result is promising for applications for spintronic devices.

In summary, we have studied the spin injection and detection in the $F1/N/F2$ structure, and derived an expression for the spin accumulation signal which covers from the metallic to the tunneling regime. This enables us to resolve the recent controversy of spin injection and detection experiments. Extending the result to a superconducting device, we have found that the signal is strongly enhanced below T_c, because superconductors become a low carrier system for spin transport by opening of the gap and a larger spin splitting is required for carrying the same spin current. Our finding can be tested in superconducting devices such as Co/I/Al/I/Co by lowering temperature below T_c. A large spin accumulation signal is also expected in semiconductor devices.

This work was supported by a Grant-in-Aid for Scientific Research from MEXT and CREST.

[1] *Spin Dependent Transport in Magnetic Nanostructures*, edited by S. Maekawa and T. Shinjo (Taylor and Francis, London and New York, 2002).

[2] A.G. Aronov, Pis'ma Zh. Eksp Teor. Fiz. **24**, 37 (1976) [JETP Lett. **24**, 32 (1976)]; Zh. Eksp. Teor. Fiz. **71**, 371 (1976) [JETP **44**, 193 (1976)]; A. G. Aronov and G.E. Pikus, Fiz. Tekh. Poluprovodn. **10**, 1177 (1976) [Sov. Phys. Semicond. **10**, 698 (1976)].

[3] M. Johnson and R.H. Silsbee, Phys. Rev. Lett. **55**, 1790 (1985); **60**, 377 (1988); M. Johnson, *ibid.* **70**, 2142 (1993).

[4] F.J. Jedema, A.T. Filip, and B.J. van Wees, Nature (London) **410**, 345 (2001); cond-mat/0207641 (unpublished).

[5] F.J. Jedema, H.B. Heersche, A.T. Filip, J.J.A. Baselmans, and B.J. van Wees, Nature (London) **416**, 713 (2002).

[6] Y. Otani *et al.*, J. Magn. Magn. Mater. **239**, 135 (2002).

[7] Y. Ohno *et al.*, Nature (London) **402**, 790 (1999).

[8] R. Fiederling *et al.*, Nature (London) **402**, 787 (1999).

[9] V.A. Vas'ko *et al.*, Phys. Rev. Lett. **78**, 1134 (1997).

[10] Z.W. Dong *et al.*, Appl. Phys. Lett. **71**, 1718 (1997).

[11] C.D. Chen, Watson Kuo, D.S. Chung, J.H. Shyu, and C.S. Wu, Phys. Rev. Lett. **88**, 047004 (2002).

[12] A. Brataas, Yu.V. Nazarov, and G.E.W. Bauer, Phys. Rev. Lett. **84**, 2481 (2000).

[13] M. Johnson, Nature (London) **416**, 809 (2002); F.J. Jedema, A.T. Filip, and B.J. van Wees, *ibid.* **416**, 810 (2002).

[14] S.D. Steenwyk, S.Y. Hsu, R. Loloee, J. Bass, and W.P. Pratt, J. Magn. Magn. Mater. **170**, L1 (1997); S. Dubois *et al.*, Phys. Rev. B **60**, 477 (1999).

[15] P.C. van Son, H. van Kempen, and P. Wyder, Phys. Rev. Lett. **58**, 2271 (1987).

[16] T. Valet and A. Fert, Phys. Rev. B **48**, 7099 (1993).

[17] A. Fert and S.F. Lee, Phys. Rev. B **53**, 6554 (1996).

[18] S. Hershfield and H.L. Zhao, Phys. Rev. B **56**, 3296 (1997).

[19] E.I. Rashba, Phys. Rev. B **62**, R16 267 (2000); Eur. Phys. J. B **29**, 513 (2002).

[20] A. Fert and H. Jaffrès, Phys. Rev. B **64**, 184420 (2001).

[21] G. Schmidt, D. Ferrand, L.W. Molenkamp, A.T. Filip, and B.J. van Wees, Phys. Rev. B **62**, R4790 (2000).

[22] The mismatch arises from those in length and area ($\lambda_N \gg \lambda_F$, $A_J \gg A_N$), not in the resistivity as in Refs. 19–21.

[23] R.J. Soulen, Jr. *et al.*, Science **282**, 85 (1998).

[24] $\rho_N=1.4\ \mu\Omega$ cm, $\lambda_N=1\ \mu$m, and $A_N=100\times50$ nm^2.

[25] $\rho_N=6\ \mu\Omega$ cm, $\lambda_N=0.65\ \mu$m, and $A_N=250\times50$ nm^2.

[26] M. Johnson and J. Byers (unpublished).

[27] S. Takahashi, H. Imamura, and S. Maekawa, Phys. Rev. Lett. **82**, 3911 (1999).

[28] J. Clarke, Phys. Rev. Lett. **28**, 1363 (1972); M. Tinkham and J. Clarke, *ibid.* **28**, 1366 (1972).

[29] T. Yamashita, S. Takahashi, H. Imamura, and S. Maekawa, Phys. Rev. B **65**, 172509 (2002).

[30] J. Bardeen, G. Rickayzen, and L. Tewordt, Phys. Rev. **113**, 982 (1959).

[31] S. Takahashi, T. Yamashita, H. Imamura, and S. Maekawa, J. Magn. Magn. Mater. **240**, 100 (2002).

[32] $\chi_s(T)=2\int_\Delta^\infty(E/\sqrt{E^2-\Delta^2})\{-[(\partial f_0(E)/\partial E)]\}dE$, whose asymptotic values are $1-[7\zeta(3)/4\pi^2](\Delta/k_BT)^2$ near T_c and $(\pi\Delta/2k_BT)^{1/2}\exp[-\Delta/k_BT]$ well below T_c.

[33] S. Takahashi and S. Maekawa, Phys. Rev. Lett. **88**, 116601 (2002).

[34] Y. Yafet, Phys. Lett. A **98**, 287 (1983).

[35] J.M. Kikkawa and D.D. Awschalom, Phys. Rev. Lett. **80**, 4313 (1998).

[36] F. Matsukura, H. Ohno, A. Shen, and Y. Sugawara, Phys. Rev. B **57**, 2037 (1998).